ANL-6935

Argonne National Laboratory

SOME CONSIDERATIONS ON THE MELTDOWN PROBLEM FOR FARET

by

P. J. Persiani, A. Watanabe,
U. Wolff, S. Grifoni, and B. Warman

Printed in USA. Price $2.00. Available from the Clearinghouse for Federal Scientific and Technical Information, National Bureau of Standards, U. S. Department of Commerce, Springfield, Virginia

ANL-6935
Reactor Technology
(TID-4500, 37th Ed.)
AEC Research and
Development Report

ARGONNE NATIONAL LABORATORY
9700 South Cass Avenue
Argonne, Illinois 60440

SOME CONSIDERATIONS ON THE MELTDOWN PROBLEM FOR FARET

by

P. J. Persiani, A. Watanabe, U. Wolff,
S. Grifoni, and B. Warman

Reactor Physics Division

September 1964

Operated by The University of Chicago
under
Contract W-31-109-eng-38
with the
U. S. Atomic Energy Commission

TABLE OF CONTENTS

	Page
ABSTRACT	7
I. INTRODUCTION	7
A. General	7
B. Analytical Consideration	8
C. Energy Available to Do Work	9
II. DESCRIPTION OF REACTOR MELTDOWN CODE (ANL 1891/RP)	10
III. DETAILED ANALYSES FOR SMALL CORE EXCURSIONS	12
A. Ramp Insertions	12
B. Small Reactivity Insertions	17
IV. DETAILED ANALYSES FOR ZONED CORE EXCURSIONS	20
A. Ramp Insertions	20
B. Small Reactivity Insertions	24
V. GENERAL COMMENTS	26
REFERENCES	27

LIST OF FIGURES

No.	Title	Page
1.	Reactivity of Collapse vs. Change in Core Height of Reference Cores	11
2.	Doppler Reactivity vs. Temperature Rise for Reference Cores	12
3.	Inverse Power Period vs. Time for Ramp Reactivity Input of \$3/sec in Reference Small Core. (Curves terminate when 87.5% of core has melted)	15
4.	Reactivity of Collapse vs. Per Cent of Core Meltdown for Reference Small Core	15
5.	Inverse Power Period vs. Energy Density for Reference Small Core	16
6.	Total Energy Available vs. Inverse Power Period for Reference Cores	17
7.	Inverse Power Period, Power Density, and Energy Density vs. Time for Reference Small Core. (Doppler effect excluded)	18
8.	Averaged Sodium Coefficient per Unit of Radial Area vs. Radius for Reference Zoned Core	21
9.	Inverse Power Period vs. Time for Ramp Reactivity Input of \$10/sec in Reference Zoned Core. (Curves terminate when 87.5% of core has melted)	21
10.	Inverse Power Period and Power Density vs. Time for Ramp Reactivity Input of \$2/sec in Reference Zoned Core. (Curves terminate when 87.5% of core has melted)	21
11.	Inverse Power Period vs. Energy Density for Reference Zoned Core	23
12.	Net Reactivity Insertion, Inverse Power Period, Power Density, and Energy Density vs. Time for Reference Zoned Core. (Initial power period = 0.11 sec)	24

LIST OF FIGURES

No.	Title	Page
13.	Net Reactivity Insertion, Inverse Power Period, Power Density, and Energy Density vs. Time for Reference Zoned Core. (Initial power period = 0.55 sec)	25
14.	Net Reactivity Insertion, Inverse Power Period, Power Density, and Energy Density vs. Time for Reference Zoned Core. (Initial power period = 1.7 sec)	25
15.	Inverse Power Period, Power Density, and Energy Density vs. Time for Reference Zoned Core. (Collapse of fuel in test zone only)	25

LIST OF TABLES

No.	Title	Page
I.	Summary of Meltdown Studies - Reference Small Core	13
II.	Calculated Average Doppler Coefficient as a Function of Temperature	14
III.	Summary of Meltdown Studies - Reference Zoned Core	19

SOME CONSIDERATIONS ON THE MELTDOWN PROBLEM FOR FARET

by

P. J. Persiani, A. Watanabe, U. Wolff,
S. Grifoni, and B. Warman

ABSTRACT

The reactor kinetics for a variety of positive reactivity-insertion rates and the effects from temperature-dependent negative reactivity feedbacks of a series of incidents which may lead to core melting have been studied. A Reactor Meltdown program was used to couple the dynamics of melting and subsequent collapsing of the core using the reactor kinetics equation.

I. INTRODUCTION

The FARET[1-3] facility is designed to accommodate a variety of fast reactor configurations, compositions, sizes, and experiments. The safety analysis for a series of specific cases would be formidable. To overcome this difficulty, the accidental reactivity insertion culminating in a reactor meltdown have been studied for two typical core loadings. The reference cores considered are: (1) the small core loading which is proposed for the Engineering Performance experiments, and (2) the zoned core loading which is planned for the Reactor Physics and Safety phase of the FARET program. The compositions and dimensions of these systems may be found in References 2 and 3.

A. General

The reactor kinetics for a variety of positive reactivity-insertion rates and the effects from temperature-dependent negative reactivity feedbacks on a series of incidents which may lead to core melting have been studied. The study of core-meltdown conditions was made in an attempt to provide a more realistic estimate of the energy yield from a reactor incident.

The range of external reactivity-insertion rates studied for the two systems were those considered to be associated with credible or near-credible conditions for FARET. For example, the ramp insertions would

include dropping of a fuel subassembly, unplanned removal of a control rod, and expulsion of (or sudden loss of) sodium coolant. Small reactivity insertions which result in a slow power rise until the fuel eventually melts and collapses were also included. These conditions could be associated with possible startup accidents, as well as loss of bulk coolant or coolant flow.

B. Analytical Consideration

The reactor incidents considered are assumed to terminate only by disassembly of the core. The analysis is separated into two phases: reactivity insertion and core disassembly.

In the disassembly phase the estimate of energy yield and explosive force of a variety of hypothetical nuclear incidences is made by use of the AX-1 code.[4] The input information needed for this computation, besides the usual reactor parameters and equations of state, is the inverse power period at the start of disassembly. The energy yield is very sensitive to this parameter, which in turn is dependent on the reactivity-insertion rate during the initial stages of disassembly.

The objective of the second phase was to estimate the maximum inverse power period for more realistic, initial reactivity-insertion rates. In this respect, the reactivity insertion eventually resulting from core melting was based on the model in which the core collapses under gravity in a time- and space-wise continuous manner. It was further assumed that as the fuel collapses, it is redistributed over the new core configuration by displacing the coolant.

This "continuous reactivity" (core-slumping) analysis is a departure from the "reactivity threshold" model, which assumes that approximately the upper half of a molten core drops as a single unit into a somewhat more densified lower core region. This most unlikely and extreme situation has been used in the studies of nuclear accidents in fast reactors,[5,6] although the authors do not necessarily give credence to such a model.

The values of the degree and the amount of core which densifies and reassembles as indicated above are questionable, and counter arguments as to the credence of this model have been advanced by Bethe.[7] The more reasonable situation is advanced in which the fuel as it is molten and comes in contact with sodium will vaporize the sodium which, in turn, will expel the molten fuel. This probably inhibits any extensive, abnormally high concentration of fuel from forming in the lower portion of the core. This appears to be a reasonable assignment of events for the case of rapid power rises in which the fuel becomes molten in tenths of msec before expelling the coolant.

The situation differs in the case of a slow power rise during which the coolant is boiled off before the fuel-melting process begins. However, the credibility of the "reactivity threshold" model remains questionable for the following reasons. To rearrange the core and create conditions for the "reactivity threshold" model to be valid would probably require much more than 100 msec. The time required for complete melting of the fuel from start of melt is of the order of tens of msec. During the intervening time between melting in situ and rearrangement of core configuration, it can be argued that some reactivity is inserted by collapse under gravity. This would lead to power periods of several msec. With such periods, the molten fuel could vaporize and create pressures within tens of msec which would tend to inhibit the formation of the extremely pessimistic geometrical configuration suggested by the "reactivity threshold" model.

The assumption made here is that the collapsing of a molten core would result in a positive reactivity insertion during the early stages of collapse. It is during this phase that a "continuous reactivity" model would appear to be more appropriate. For conceivable realistic accidents which could result in a partial core meltdown, this model, at present, is considered to be more appropriate for the purpose of estimating the energy yield.

In the FARET analysis, the collapsing of the core was allowed to proceed until the total energy input reached a value of 2×10^4 Joules/cc of fuel, whereupon the core started to disassemble. This may be taken as the energy required to vaporize the fuel. The inverse power period corresponding to this energy was then used as the input parameter for the computation of the energy yield (AX-1 Code). This approach affords a more detailed evaluation of core conditions and parameters which may exist during meltdown and reassembly, and thus provides a more reasonable estimate of the energy yields.

C. Energy Available to Do Work

The energy yield pertinent to this safety analysis is defined as the amount of the total energy available which is converted into energy to do work. This quantity was obtained by first determining the total energy yield for a given inverse power period and then multiplying this quantity by the factor (0.60) x (0.10). The first term (0.60) is based on a slightly less pessimistic equation of state used in the disassembly code (see Section III, pp. 16-17), which essentially allows a slightly more dense configuration at the time of disassembly, or an equivalently slightly lower temperature at which disassembly starts.

The second term (0.10) is an estimate that a reactor system is only 10% efficient in converting the total heat energy into mechanical energy. The fraction of the total energy which is available for work includes the kinetic energy and the volume-integrated pressure at the end of the excursion. From the AX-1 computation, an estimate of this quantity was made for the zoned system by use of the overly pessimistic inverse power period $\alpha = 0.01/\mu$sec. For this case, the maximum energy available to do work was computed to be about 8% of the total energy yield. Since further analytical work is required to establish such a value more firmly, the efficiency factor of 10% was used to convert the total energy into mechanical energy.

II. DESCRIPTION OF REACTOR MELTDOWN CODE (ANL 1891/RP)

The Reactor Meltdown Code was used to investigate the dynamic behavior of the two reference cores following a positive reactivity insertion, and the corresponding positive and/or negative reactivity feedbacks from temperature-dependent mechanisms, and the degree of core collapse after melting had started. The program couples the dynamics of melting and collapsing of the core with the reactor kinetics equation. The models used for the various changes of reactivity are incorporated into three basic types of reactivity insertions or feedbacks.

First is the externally applied reactivity, R_x. Straight ramp insertions or ramp insertions up to a time t_0 may be allowed. The forms of the equations are

$$R_x(t) = A_{x1} + A_{x2}t \text{ for } t \leq t_0; \tag{1}$$

$$R_x(t) = A_{x1} + A_{x2}t_0 \text{ for } t > t_0, \tag{2}$$

where A_{x1} and A_{x2} are arbitrary coefficients which define the rates of ramp insertion.

The second type of reactivity change considered is that which is a function of core displacement, e.g., the collapsing of the core. This is labelled R_c. The equations are of the form

$$R_c = A_{c1}(\Delta H) + A_{c2}(\Delta H)^2, \qquad (3)$$

where ΔH is the change in active core height, and A_{c1} and A_{c2} are collapse coefficients chosen to fit a predetermined curve.

The reactivity addition due to core collapse is determined from a series of static reactor calculations as a function of reactor height. For the model used in these computations it was assumed that the melted segment of the fuel is uniformly distributed over the remaining core height, with an equal volume displacement of coolant.

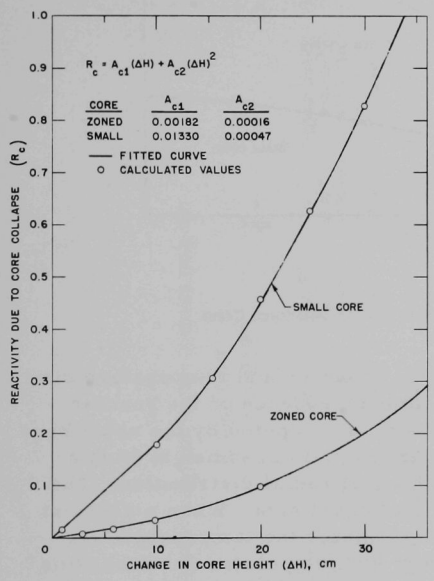

Figure 1

Reactivity of Collapse vs. Change in Core Height of Reference Cores

Figure 1 shows the reactivity of collapse as a function of change in core height for the two reference cores.

The time dependence of collapse is determined through a modified gravitational equation of motion:

$$\frac{d^2H}{dt^2} + \xi \frac{dH}{dt} = -g, \qquad (4)$$

which allows the collapse to occur at an acceleration less than g. The "dynamical friction" term

$$\xi \frac{dH}{dt}$$

is included to account for cores containing closely packed fuel elements. An assemblage of fuel pins may behave quite differently than a molten isolated pin. For purposes of the FARET analysis, the coefficient was estimated to be 0.3. This estimate was based on a single oxide-fuel pin experiment in the TREAT reactor.

The third reactivity insertion considered is dependent on the change of temperature, e.g., fuel and coolant and Doppler effects. The code at present includes only the Doppler effect, R_D. The temperature dependence of the Doppler reactivity is obtained from a series of static calculations involving Doppler-broadened cross sections for several fuel temperatures.

Figure 2 shows the temperature dependence of the Doppler reactivity for the two reference cores. A good fit was obtained with the relation:

$$R_D = A_{D1}[1 - \exp(-A_{D2}\,\Delta\theta)], \tag{5}$$

where $\Delta\theta$ is the averaged rise of fuel temperature, and A_{D1} and A_{D2} are coefficients chosen to obtain a good fit.

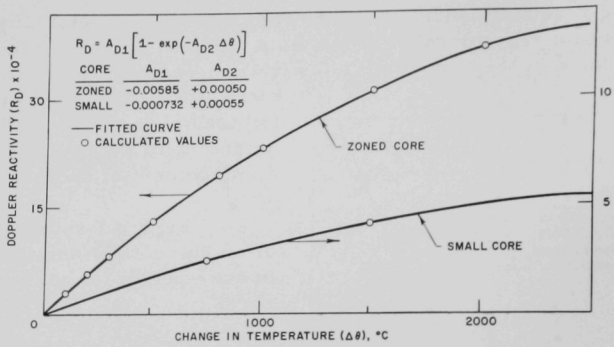

Figure 2

Doppler Reactivity vs. Temperature Rise for Reference Cores

The code permits the computation of power and temperature distributions at each time interval. The time dependence of the reactor power, with one group of delayed neutrons, is computed by the usual neutron kinetics equations. The power distribution is assumed to have a cosine shape in the axial direction, with a flat radial distribution. The core is divided axially into 40 segments of equal size. When a segment melts and collapse occurs, the code recalculates the temperature distribution over the new height. The power and temperature at each time are used to compute the reactivity feedback through the equations defined above. The reactivity insertions are then fed back into the neutron kinetics equations.

III. DETAILED ANALYSES FOR SMALL CORE EXCURSIONS

A. Ramp Insertions

Meltdown studies have been made for a series of positive reactivity-insertion rates ranging from \$3/sec to \$20/sec. The results for the small core are summarized in Table I. The range of insertion rates was established on the basis of the following considerations:

Table I

SUMMARY OF MELTDOWN STUDIES - REFERENCE SMALL CORE

$\beta_{eff} = 0.00274$

$\ell = 0.655 \times 10^{-6}$

External Reactivity, $/sec	Ramp Break, sec	Time Melting Starts, sec	Melting Time, sec		R_{net} Melting Starts	R_{net} Melting		$\Delta k_{avg}/\Delta T$ during Melting	α, μsec^{-1} at 87.5% Melt	Power Density, watts/cm^3 at 87.5% Melt	Energy Density, joules/cc at 87.5% Melt	Average Doppler Coefficient, $\Delta k/\Delta T$ (750-2500°K)
			50% Melt	87.5% Melt		50% Melt	87.5% Melt					
3	0.608	0.388200	0.006058	0.010010	0.002733	0.002965	0.003320	0.0586	1.0×10^{-3}	6.7×10^{6}	1.7×10^{4}	-0.22×10^{-6}
3	0.608	0.367235	0.002800	0.007634	0.002790	0.002844	0.003146	0.0466	7.0×10^{-4}	4.3×10^{6}	1.6×10^{4}	-0.11×10^{-6}
3	0.608	0.352648	0.001482	0.003200[a]	0.002899	0.002926	0.003000[a]	0.0315[a]	4.6×10^{-4}[a]	3.1×10^{6}[a]	1.5×10^{4}[a]	0
4	0.456	0.291318	0.004714	0.009382	0.002735	0.002872	0.003267	0.0567	9.2×10^{-4}	5.7×10^{6}	1.6×10^{4}	-0.22×10^{-6}
4	0.456	0.277518	0.002282	0.006534	0.002813	0.002853	0.003077	0.0404	5.7×10^{-4}	4.3×10^{6}	1.7×10^{4}	-0.11×10^{-6}
5	0.365	0.233250	0.003707	0.008042	0.002738	0.002837	0.003103	0.0454	7.1×10^{-4}	3.5×10^{6}	1.5×10^{4}	-0.22×10^{-6}
5	0.365	0.217272	0.000950	0.0017[a]	0.002977	0.002994	0.003055[a]	0.0170[a]	4.6×10^{-4}[a]	4.3×10^{6}[a]	1.3×10^{4}[a]	0
20	0.22	0.060778	0.000905[a]	0.0017[a]	0.003333	0.003382[a]	0.003427[a]	0.0549	1.0×10^{-3}[a]	1.9×10^{7}[a]	2.1×10^{4}[a]	0

[a]Extrapolated values.

Note: In all cases, $P_0 = 1.2 \times 10^3$ watts/cm^3.

Core Volume = 41.7 liters.

(1) The control rod worth was estimated to be 0.004 $\Delta k/ft$. By assuming a control rod removal rate of 6 ft/sec, we obtained a positive reactivity-insertion rate of 0.0243 $\Delta k/sec$. With a value for β_{eff} of 0.00274, the rate is equivalent to approximately \$9/sec.

(2) The reactivity insertion rate of \$20/sec was obtained by using an average worth of 0.009 $\Delta k/ft$ for the fuel subassembly, and an average free-fall velocity of 6 ft/sec through the core.

The results of the meltdown computation indicate (see Table I) that for reactivity-insertion rates below \$5/sec, the melting process will begin about 200 to 400 msec after the start of the external insertion. The time for 50% and 87.5% of the core to melt ranges from 1 to 10 msec.

When the negative feedback of the Doppler coefficient is neglected, the time required to melt 87.5% of the core is 1.7 msec and 3.2 msec for reactivity-insertion rates of \$5/sec and \$3/sec, respectively (see Table II). These are the shortest melting times involved, and the reactivities attained are the largest. For the case of an insertion rate of \$5/sec, the reactivity due to collapse is small, so that during the melting process the rate of reactivity associated with the \$5/sec insertion is not altered. However, for the lower ramp insertion rate of \$3/sec, the reactivity due to collapse is effective in increasing the rate during the melting process to approximately \$10/sec (see Table I). Therefore, it appears that the lower rates of external reactivity insertion could lead to higher rates of insertion during the melting and reassembly processes.

Table II

CALCULATED AVERAGE DOPPLER COEFFICIENT AS A FUNCTION OF TEMPERATURE

Temperature Range, °K	Doppler Coefficient, (Δk_{eff}/°K) x 10^{-6}	Temperature Range, °K	Doppler Coefficient, (Δk_{eff}/°K) x 10^{-6}
Small Core		Zoned Core (Coefficient in test zone only)	
300-750	-0.43	300-750	-1.53
300-1500	-0.37	300-1500	-1.08
300-2500	-0.30	300-2500	-0.84
750-1500	-0.33	750-1500	-0.81
750-2500	-0.26	750-2500	-0.67
1500-2500	-0.22	1500-2500	-0.56

To study the latter effect, a series of computations were made with the introduction of negative Doppler coefficients of different magnitudes. The temperature-dependent negative feedback was introduced to offset the initial positive reactivity insertion. The resulting rate of insertion during the melting process confirmed the conclusions stated for the no-Doppler case, that is, in the small-core analysis, a negative feedback having these orders of magnitude could result in a greater reactivity contribution from the collapsing of the core. The Doppler effect can be seen in Figure 3, where the inverse power period, α, is plotted as a function of time. The magnitude of the Doppler effect is not large enough to effect a reactor shutdown. In Figure 4 are presented the collapse reactivity for varying degrees of melt in systems computed with and without the Doppler effect.

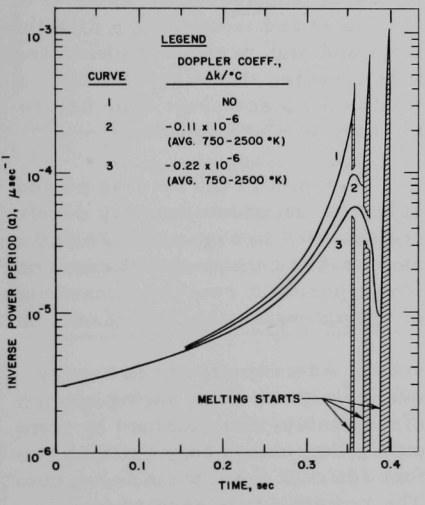

Figure 3

Inverse Power Period vs. Time for Ramp Reactivity Input of $3/sec in Reference Small Core. (Curves terminate when 87.5% of core has melted)

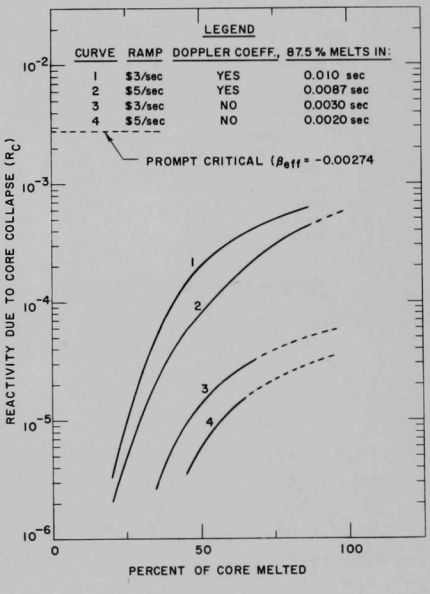

Figure 4

Reactivity of Collapse vs. Per Cent of Core Meltdown for Reference Small Core

A ramp insertion rate of $20/sec will cause the core to start melting 60 msec after the initial insertion. In about 2 msec, the core would be 87.5% molten. The short time interval of melting would not allow any significant reactivity to be inserted by collapse. The inverse power period is minimum for this case, and the average reactivity-insertion rate during melting is the same as the initial input.

The effect of the negative feedback is to increase the melting time and, hence, to allow a greater degree of core collapse to occur. In all cases studied, the net reactivity did not exceed $0.22 above prompt critical when 87.5% of the core was molten.

The shortest power period occurred with the maximum negative feedback. The inverse periods α at 87.5% melt for the cases studied are included in Table I.

The meltdown code computes the total energy input during the excursion. At 87.5% melt, the total energy input was of the order of 2×10^4 Joules/cc of fuel (see Table I), or 4.2×10^8 Joules (1×10^8 cal) for the entire 41.7-liter core. The energy required to sublimate the oxide fuel in the core was computed to be 4×10^8 Joules (1×10^8 cal) when a heat of sublimation of 2000 Joules/gm was assumed.[8,9] Therefore, when 87.5% of the core is in this highly superheated liquid or molten state, the energy input is of the same order of magnitude as the energy required to vaporize the core. Consequently, because of the power and temperature distributions and high pressures generated, it is expected that disassembly would take place some time before the core is 87.5% molten.

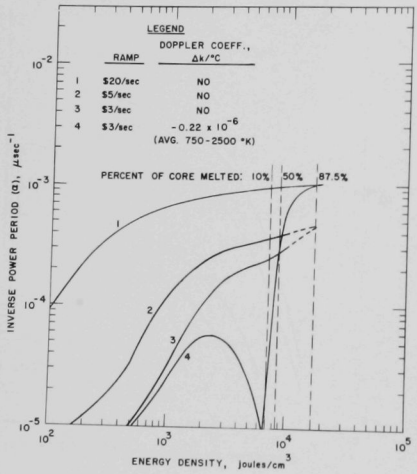

Figure 5

Inverse Power Period vs. Energy Density for Reference Small Core

A plot of the inverse period as a function of total energy density is presented in Figure 5. For all ramp cases considered, the inverse power period α reached a maximum of approximately $1 \times 10^{-3}/\mu$sec.

An estimate of the energy available to do work during core disassembly, was obtained by computing the total energy yield as a function of α from the AX-1 code. The results are presented in Figure 6. For the small core with an α of the order of $1 \times 10^{-3}/\mu$sec, the total energy yield was approximately 7×10^7 Joules (1.67×10^7 cal).

A computation was also performed in which the fuel temperature at which pressure would begin to rise in the core region was taken as 4400°C for comparison with those based on 6700°C. (A temperature of 4400°C is approximately 1000°C to 1200°C above the boiling temperature of the oxide fuel.) The energy available to do work was reduced to 60% of that at the higher temperature (6700°C), whereas the maximum kinetic

energy remained the same. This behavior appears reasonable, since reducing the temperature in the pressure equation allows the core to disassemble sooner, but the amount of total energy converted into kinetic energy remains the same. The lower temperature is equivalent to a slight increase in the core density in the equation of state used in the AX-1 computation. The density was increased from 5.2 to 6.5 gm of fuel/cc of core.

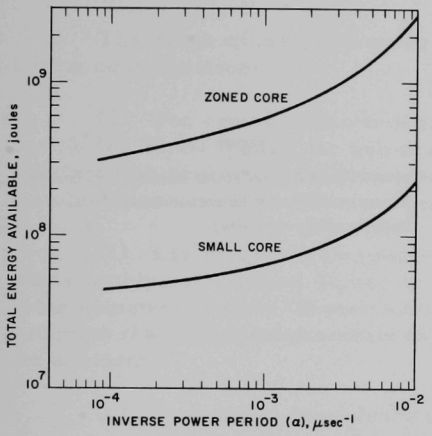

Figure 6
Total Energy Available vs. Inverse Power Period for Reference Cores

When the temperature effect upon the calculated total energy yield was taken into account, the energy available to do work for $\alpha = 0.001/\mu sec$ was reduced from 7×10^6 Joules to about 4×10^6 Joules.

B. Small Reactivity Insertions

The effects of a slow meltdown were studied in order to evaluate the type of accident in which melting of the core would occur for a period prior to prompt critical and is followed by the collapse of the core. An accident of this type might be initiated by decrease of coolant flowrate to the reactor, severe local perturbations in flow, or failure of experimental fuel subassemblies.

In order to estimate effects resulting from an accident of this type which increase the melting time, and thereby the extent of core collapse, a constant, low, inverse-power period was introduced initially. The Doppler feedback was neglected. As shown in Figure 7, the time required for 70% and 100% of the core to melt is 15.5 msec and 17 msec, respectively.

The inverse-power period attained due to core collapse is about 2 to 3 x $10^{-3}/\mu$sec at the input energy density of 2 x 10^4 Joules/cc of fuel. The conditions for energy yields in this "slow meltdown" accident are quite similar to the ramp-insertion cases. Work-energy yields of about 6 x 10^6 Joules can be expected.

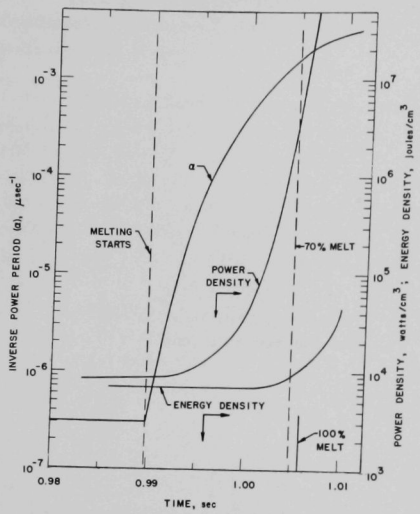

Figure 7

Inverse Power Period, Power Density, and Energy Density vs. Time for Reference Small Core. (Doppler effect excluded)

In addition, if the initial power level is low, the inverse-power period would increase by 10%, and the work energy would increase to about 7 x 10^6 Joules. It should be noted that computations indicate that energy yield is not particularly sensitive to initial power level.

IV. DETAILED ANALYSES FOR ZONED CORE EXCURSIONS

A. Ramp Insertions

Meltdown studies were performed also for a typical zoned system. Positive-reactivity ramp insertions of \$2/sec, \$10/sec, and \$20/sec were assumed. The results, with and without Doppler feedback, are presented in Table III.

The range of insertion rates was established on the basis of the following considerations:

(1) The control rod worth per linear foot of rod was estimated to be 0.00167 $\Delta k/ft$. Again, the use of a control rod removal rate of 6 ft/sec resulted in a positive reactivity-insertion rate of 0.01 $\Delta k/sec$, or approximately \$2/sec, when a value for β_{eff} of 0.0066 was assumed.

(2) The range of reactivity-insertion rates for the free fall of a fuel subassembly varied from \$6/sec to \$20/sec, with a more probable rate being somewhat lower. These values were based on the pessimistic assumption that a fuel subassembly of maximum worth would be involved in the accident.

(3) The spatial dependence of the sodium expansion coefficient for the zoned system is presented in Figure 8. The estimated magnitude and sign indicated that a postulated loss of coolant in only the test zone could result in melting of the fuel. If it may be assumed that the sodium could be expelled from the test zone in from 600 to 30 msec, the average reactivity-insertion rate would be in the range from \$1/sec to \$20/sec.

The magnitudes of the Doppler coefficients used in the code computations were taken as 1/3 of the calculated values listed on the figures and tables. This reduction was made since (1) allowances were made for the uncertainty in the magnitude which could be associated with the actual experiment, and (2) the use of the full Doppler coefficient resulted in reducing the excursion power levels to values which could be interpreted as a reactor shutdown. For the ramp cases studied, the positive reactivities resulting from core collapse were negligible. However, in the case of \$2/sec ramp insertion, the contribution of collapse was greater by a factor of 3 to 4 than in the \$10/sec case.

As shown in Table III, the existence of the Doppler effect resulted in reducing the external input during the melting process. In the case of \$2/sec ramp insertion, the $\Delta k/\Delta T$ during melt became \$1.40/sec; for the \$10/sec ramp, the rate became \$3/sec. The respective inverse-power periods were lower in both cases than for the case in which the Doppler effect was not considered.

Table III

SUMMARY OF MELTDOWN STUDIES - REFERENCE ZONED CORE

$\beta_{eff} = 0.0066$

$\ell = 0.89 \times 10^{-6}$

External Reactivity, $/sec	Ramp Break, sec	Time Melting Starts, sec	Melting Time, sec		R_{net} Melting Starts	R_{net} Melting		$\Delta k_{avg}/\Delta T$ during Melting	α, μsec^{-1} at 87.5% Melt	Power Density, watts/cm^3 at 87.5% Melt	Energy Density, joules/cc at 87.5% Melt	Average Doppler Coefficient, $\Delta k/\Delta T$ (750-2500°K)
			50% Melt	87.5% Melt		50% Melt	87.5% Melt					
2	1.00	0.52648	0.00126	0.0024[a]	0.006924	0.006942	0.006958[a]	0.014	4.3×10^{-4}[a]	5.8×10^{6}	1.6×10^{4}[a]	0
2	1.00	0.58523	0.01203	0.02083	0.006608	0.006774	0.006803	0.00934	2.7×10^{-4}	3.1×10^{6}	2.0×10^{4}	-0.64×10^{-6}
10[b]	0.40	0.12398	0.00070[a]	0.0012	0.008156	0.008282[a]	0.008235[a]	0.066	1.9×10^{-3}[a]	4.6×10^{7}[a]	2.8×10^{4}[a]	0
10	0.40	0.11332	0.00060	0.00081[a]	0.007454	0.007492	0.007507[a]	0.066	1.2×10^{-3}[a]	1.5×10^{7}[a]	1.7×10^{4}[a]	0
10	0.40	0.11509	0.00383	0.01043	0.006533	0.006676	0.006764	0.022	2.2×10^{-4}	3.3×10^{6}	2.3×10^{4}	-0.64×10^{-6}
20[c]	0.152	0.056885	0.000456	0.00080[a]	0.007482	0.007542	0.007587[a]	0.132	1.2×10^{-3}[a]	5.9×10^{7}[a]	1.5×10^{4}	0
20	0.152	0.060	-	-	0.007900[a]	-	-	0.132[a]	2.0×10^{-3}	-	-	0
2[d]	1.00	0.51872	0.002366	0.00567	0.006823	0.006858	0.006922	0.0175	3.7×10^{-4}	7.7×10^{5}	3.1×10^{3}	0
10[d]	0.40	0.11121	0.000889	0.001755	0.007315	0.007378	0.007431	0.0661	9.7×10^{-4}	3.1×10^{6}	3.8×10^{3}	0
10[d]	0.40	0.11194	0.000853	0.002263	0.007069	0.007050	0.007030	-0.0172	5.2×10^{-4}	1.7×10^{6}	3.3×10^{3}	-0.64×10^{-6}

[a] Extrapolated values.

[b] $P_0 = 1.4 \times 10^{-4}$ watts/cm^3; in all other cases, $P_0 = 1.4 \times 10^{2}$ watts/cm^3.

[c] $P_0 = 3.13 \times 10^{3}$ watts/cm^3.

[d] Melting temperature of fuel 1150°C. Core volume = 460 liters.

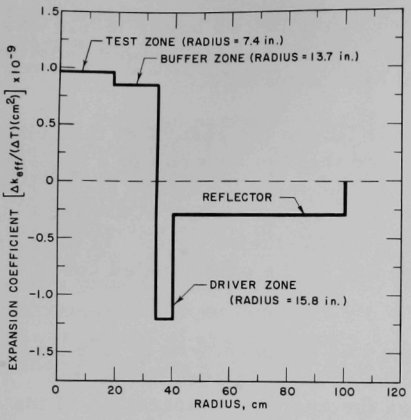

Figure 8

Averaged Sodium Coefficient per Unit of Radial Area vs. Radius for Reference Zoned Core

In all cases for which the Doppler effect was neglected, the rate of reactivity insertion during melting remained the same as the external input.

The overall conclusion which can be made for the zoned system is that for the external insertion rates studied, the fuel melted, but negligible reactivity was introduced by the collapsing process. In comparison with the small core, the zoned core was of greater height, and the worth of collapse per unit height was of less importance. It should be noted that the maximum net reactivity insertion did not exceed $0.25 above prompt critical.

The inverse-power periods as a function of time are presented in Figures 9 and 10. In the two cases for which the Doppler effect was included, the inverse-power period became negative, but the magnitude was not large enough to reduce the power level to zero. In Figure 10, the power versus time is included to observe the effect of the Doppler. The power was reduced somewhat, but then increased and the core melted.

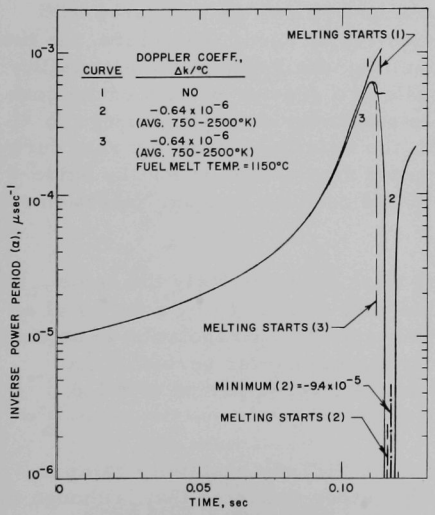

Figure 9

Inverse Power Period vs. Time for Ramp Reactivity Input of $10/sec in Reference Zoned Core. (Curves terminate when 87.5% of core has melted)

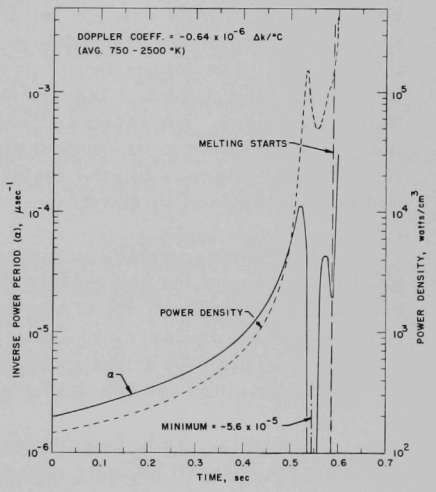

Figure 10

Inverse Power Period and Power Density vs. Time for Ramp Reactivity Input of $2/sec in Reference Zoned Core. (Curves terminate when 87.5% of core has melted)

The inverse period for the \$20/sec ramp for two power levels was studied. When the reactivity insertion was initiated at high power densities, the inverse-power period was decreased by a factor of 2.

The last three cases listed in Table III are the results of the melt-down code analyses in which it was assumed that the severity of a nuclear accident is due primarily to the behavior of the metallic driver zone. For these cases, the melting temperature of the uranium metal (1150°C) was used. Hereafter, these cases are identified as metallic-fueled cores. In the former cases, the melting temperature used was that of the oxide-fueled cores (2750°C).

For the metallic-fueled cores, the fuel temperatures at an energy input of 2×10^4 Joules/cc of fuel were usually low. In such cases, the inverse-power period used was that when the average temperature of the fuel was approximately equal to the boiling temperature of the metal fuel (4100°C). For the oxide-fueled cores, boiling temperatures of ~3300°C were attained when the energy input of 2×10^4 Joules/cc of fuel was reached. For the ramp insertions studied, the inverse-power period was essentially insensitive to either energy input or average fuel temperature. For this preliminary analysis, the energy input was considered appropriate.

When the case for the \$2/sec reactivity insertion rate was compared with a \$2/sec ramp associated with the oxide fuel, the metallic-fueled core was found to start to melt about 7 msec sooner. The net reactivity inserted at the start of melt was \$0.035 above prompt critical, as compared with \$0.052 above prompt critical for the oxide-fueled core. Therefore, the time required to attain the same degree of melting was longer for the metallic-fueled core. The longer time interval allows a greater portion of the core to collapse and, hence, a larger positive reactivity insertion during the melting process. As shown in Table III, the reactivity insertion rate during melt was the same as the externally applied rate of \$2/sec for the oxide-fueled core, whereas for the metallic-fueled core the average insertion rate had been increased to \$2.60/sec.

The power periods in both cases were approximately the same. The total energy input for the metallic-fueled core was lower by a factor of approximately 5 when 87.5% of the core had melted. Extrapolation to an energy input of 2×10^4 Joules/cc of fuel gave an inverse-power period of 6×10^{-4} μsec. This is a slight increase over the inverse period of $4.3 \times 10^{-4}/\mu$sec obtained for the oxide-fueled core.

A similar study was performed for a \$10/sec reactivity ramp insertion rate without Doppler effects. This study indicated that, although the required melting time increased, the initially applied reactivity insertion rate still predominated and core collapse was negligible. The total energy

input was lower by a factor of 5 than that of the oxide-fueled core. Extrapolation to an energy input of 2×10^4 Joules/cc of fuel gave an inverse-power period of $1.2 \times 10^{-3}/\mu$sec.

For comparison, the \$10/sec insertion rate cases were studied with the Doppler effect included. The results indicated that the net Doppler feedback contribution during the melting process was not sufficient to lower the net reactivity inserted as the core melts. As shown in Table III, the net reactivity was above prompt critical and decreased slightly or was constant during the melting process. In the oxide-fueled core, the net reactivity was below prompt critical and increased slightly during the melting process. Extrapolation to an energy input of 2×10^4 Joules/cc of fuel gave an inverse-power period of approximately $7 \times 10^{-4}/\mu$sec. In both cases, the reactivity added due to core collapse was negligible.

For all cases studied, the maximum inverse-power period was of the order of $2 \times 10^{-3}/\mu$sec. The average energy input was of the order of 5×10^9 Joules (1×10^9 cal). The energy required to sublimate the metal fuel in the driver zone and the oxide fuel in the test zone was about 3×10^9 Joules (7.5×10^8 cal), based on a heat of vaporization of 2000 Joules/gm.[9] The total energy input into the fuel was of the same order of magnitude as the energy required to vaporize the core.

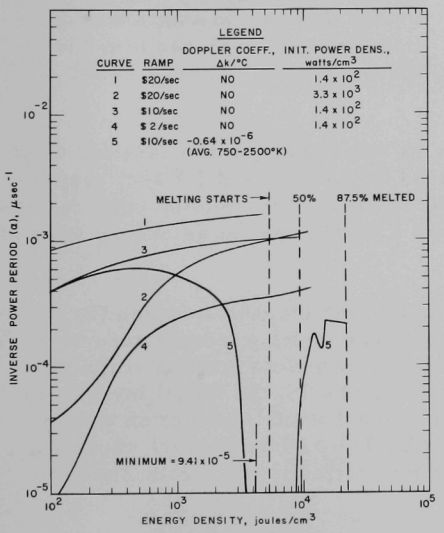

Figure 11

Inverse Power Period vs. Energy Density for Reference Zoned Core

As in the case of the small core, the core disassembly should be expected to take place some time before the core is 87.5% molten, provided that the energy input is approximately 2×10^4 Joules/cc of fuel. In Figure 11, the inverse-power period is plotted as a function of total energy input for the ramp insertions studied. For all cases, α was less than $2 \times 10^{-3}/\mu$sec.

To estimate the energy yield during core disassembly, the same procedure was followed as was used in the small-core studies. For an α of the order of $2 \times 10^{-3}/\mu$sec, the total energy yield was of the order of 7×10^8 Joules (1.7×10^8 cal).

Assuming a 10% efficiency for converting heat energy into mechanical energy, and that the core begins to disassemble when the fuel vapor temperature is about 1000°C to 1200°C above the boiling point, the energy available to do work was estimated to be about 5×10^7 Joules.

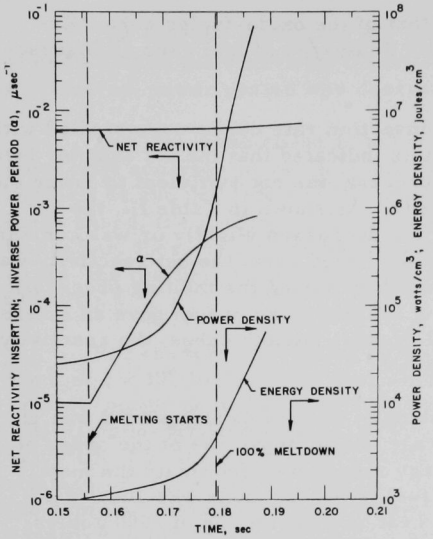

Figure 12

Net Reactivity Insertion, Inverse Power Period, Power Density, and Energy Density vs. Time for Reference Zoned Core. (Initial power period = 0.11 sec)

B. Small Reactivity Insertions

In order to observe the effects of a "slower meltdown" and a higher degree of core collapse, a constant inverse-power period of $9 \times 10^{-6}/\mu$sec was initially introduced into the zoned system. The melting temperature used was that of the metal driver. As shown in Figure 12, the time required for 100% of the core to melt is about 23 msec. The input energy density, 2×10^4 Joules/cc of fuel, was reached in 29 msec. The inverse-power period at this time is approximately $1 \times 10^{-3}/\mu$sec.

However, extrapolation to a fuel temperature of about 4100°C could increase the inverse-power period to about $2 \times 10^{-3}/\mu$sec. If the higher of the two periods is used, the estimated energy yield becomes about 5×10^7 Joules. In addition, if the initial power level was low, the inverse period could increase by about 70% and the work energy would increase to about 6×10^7 Joules.

The results plotted in Figures 13 and 14 pertain to cases for which the initial power periods were increased to 0.55 sec and 1.7 sec, respectively. In both cases, the gravitational collapse of the molten core resulted in an inverse-power period of less than $2 \times 10^{-3}/\mu$sec at an energy input of about 2×10^4 Joules/cc of fuel.

Also considered was a "slow meltdown" incident in which the fuel in the test zone was allowed to collapse. The melting temperature of the oxide fuel was used. The time required for complete melting of the fuel was about 55 msec. As made evident in Figure 15, the initial inverse period of $4 \times 10^{-6}/\mu$sec was increased to about $1 \times 10^{-3}/\mu$sec at an energy density input of 2×10^4 Joules/cc of fuel. The estimated work energy in this case is about 4×10^7 Joules. For low initial power levels, the estimate is 5×10^7 Joules.

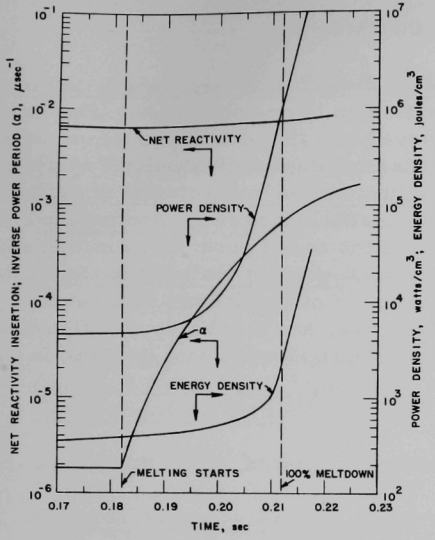

Figure 13

Net Reactivity Insertion, Inverse Power Period, Power Density, and Energy Density vs. Time for Reference Zoned Core. (Initial power period = 0.55 sec)

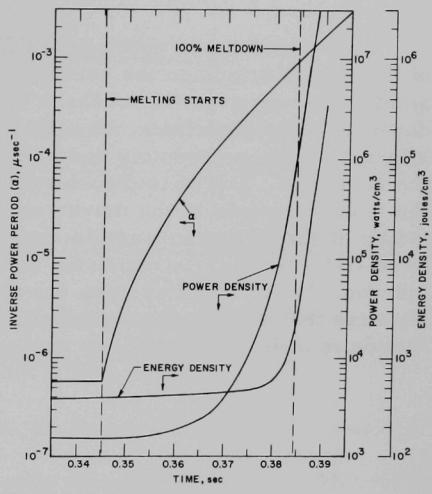

Figure 14

Net Reactivity Insertion, Inverse Power Period, Power Density, and Energy Density vs. Time for Reference Zoned Core. (Initial power period = 1.7 sec)

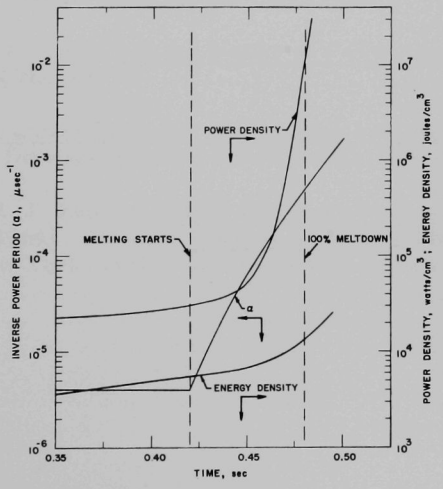

Figure 15

Inverse Power Period, Power Density, and Energy Density vs. Time for Reference Zoned Core. (Collapse of fuel in test zone only)

V. GENERAL COMMENTS

The calculated energy yields are believed to be pessimistic in view of the qualifications on the parameters used in the computations. For example, the only negative feedback employed was that due to the temperature-dependent Doppler effect. The time scales involved indicate that "delayed effects" could be operative and may, in most cases, mitigate the severity of the accidents. For example, the sodium coefficient is large and negative in the small core and in the driver section of the zoned core; this mechanism could terminate some possible excursions. It was not included in the meltdown code, that is, the expulsion or boiling-off of the sodium was not considered. In the zoned system, the metal driver has a reliable and significant negative fuel-expansion coefficient. This effect also was not included in the meltdown code.

REFERENCES

1. Interim Report: FARET EXPERIMENTAL PROGRAM, ANL-6708 (April 1963).

2. P. J. Persiani, "Reactivity Coefficient Measurements in FARET," Proceedings of the Conference on Breeding, Economics, and Safety in Large Power Reactors, ANL-6792 (Oct 1963), p. 873.

3. Preliminary Safety Analysis of the Fast Reactor Test Facility (FARET), ANL-6813 (Aug 1964).

4. D. Okrent, J. M. Cook, D. Satkus, R. B. Lazarus, and M. B. Wells, AX-1: A Computing Program on Coupled Neutronics-Hydrodynamics Calculations on the IBM-704, ANL-5977 (May 1959).

5. L. J. Koch, H. O. Monson, D. Okrent, M. Levenson, W. R. Simmons, J. R. Humphreys, J. Haugsnes, V. Z. Jankus, W. B. Loewenstein, Hazards Summary Report, Experimental Breeder Reactor-II, ANL-5719 (May 1957), and Addendum (June 1962).

6. W. J. McCarthy, Jr., R. B. Nicholson, D. Okrent, and V. Z. Jankus, Studies of Nuclear Accidents in Fast Power Reactors, Proceedings of the Second UN International Conference on the Peaceful Uses of Atomic Energy, Geneva, Switzerland, 12, 207-229 (1958).

7. Testimony of H. A. Bethe, On the Matter of Power Reactor Development Company, Docket No. 50-16.

8. J. Belle (ed.), Uranium Dioxides: Properties and Nuclear Applications, Naval Reactors, Division Reactor Development, USAEC (1961).

9. E. G. Rauh and R. J. Thorne, Vapor Pressure of Uranium, J. Chem. Phys. 22, 1414 (1954). See also Reactor Handbook (Interscience Publishers, Inc., New York, 1960), 2nd Ed., Vol. I, p. 112.